11th World Congress on Computational Mechanics (WCCM XI)
5th European Conference on Computational Mechanics (ECCM V)
6th European Conference on Computational Fluid Dynamics (ECFD VI)
E. Oñate, J. Oliver and A. Huerta (Eds)

AN INTERFACE DAMAGE MODEL DEPENDING ON THE IN-PLANE DEFORMATION

F. FREDDI[*], E. SACCO[†]

[*] Department of Civil-Environmental Engineering and Architecture
University of Parma
Viale G. P. Usberti 181/A, Italy
email: francesco.freddi@unipr.it

[†] Department of Civil-Mechanical Engineering
University of Cassino and Southern Lazio
Via G. Di Biasio 43, Cassino
email: sacco@unicas.it

Key Words: *Damage, Enriched Interface Element, Cohesive Interface, Debonding.*

Abstract. In the present work, an enhanced formulation for cohesive interface that keep into account the effect of in-plane deformations of the gluing surface is proposed. Starting from this kinematical assumption an enriched formulation of interface finite element is proposed. The enriched formulation introduces also a constitutive correlation between the in-plane deformation (elongation or confinement) of the interface and the membrane state of stress. An interface damage model which accounts for the mode I and mode II and the axial deformation of the interface is proposed starting by the use of Drucker-Prager failure criterion. Simple numerical simulations are presented in order to illustrate the capabilities of the model. In particular, the effects of mortars joints in masonry substrate reinforced with FRP is investigated.

1 INTRODUCTION

Many structural problems require the analysis of initiation and evolution of important damage phenomena. The heterogeneity of structure, or particular loading and constraint conditions, concentrate damage and macroscopic separation which are thus forced to appear in a limited number of critical zones, while the remaining parts can still be considered in elastic regime. In particular, the interfaces between different materials are important regions governing the strength and stability of structures. In fact, local ruptures and material de-cohesion develop in macroscopic fractures and separations between parts. Consequently an accurate understanding of fracture initiation and propagation has become ever more important from the serviceability and safety standpoints for structures.

This is the case of external strengthening of quasi-brittle substrates (masonry or concrete) by means of Fiber Reinforced Polymer (FRP) that has gained great importance in the last few years especially in historic and monumental buildings due to its low invasiveness, great

efficiency and low weight-to-strength ratio. In fact, debonding in FRP reinforcements is a typical failure mode [1][2].

The fracture process initiate and propagate in a narrow region (the adhesive and a thin layer of substrate cover) separating two well defined domains. These regions are often described by cohesive crack where the fracture process zone is modelled as a fictitious crack, ahead of the actual traction-free crack; the strain localization is idealized as a crack opening and sliding, related to cohesive tractions. The role of the interface is essential to the stress transfer between FRP and substrate influencing the structural behaviour in terms of stiffness, strength and failure behaviour. However in some cases, the interface presents a state of deformations that cannot be completely describe by relative displacement, for example in the presence of in-plane elongation[3], coupling between the body and interface damage [4][5] or confinement effects.

Numerical models for FRP debonding are typically based on shear stress–tangential slip interface laws that are calibrated by direct shear tests [6]. In this case, relative displacement between FRP reinforcement and substrate is lumped within the interface layer, whose constitutive law collects all compliance and non-linear contributions of adhesive and external substrate layer. This modelling approach demonstrated success for specific test configurations and design procedure, but there is still a need for models that can satisfactorily predict the debonding failure phenomena in more general cases.

The cohesive interface law is strongly influenced by boundary effects [7] and should take into account and reflect the complex behaviour and processes taking place in a substrate "compliance volume" [5]. In Figure 1, the stresses obtained numerically in the substrate and reproducing the shear test proposed in [8] for two load levels (60% and 100% of the maximum value of transmissible force P_{max}) are reported. In both cases, the process zones under the gluing surface evidence non negligible stresses σ_x, accompanying the classical τ_{xy}, that certainly influence the bonding behaviour. Moreover, this confinement effect changes and peeling stresses may appear at the extremities of the reinforcement thus leading to noticeable changes of the transmittable shear stresses.

In the present work, an enhanced formulation for cohesive interface that keep into account the effect of in-plane deformations of the gluing surface is proposed. Starting from this kinematical assumption an enriched formulation of interface finite element is proposed. In fact, the interface is commonly modelled by zero thickness finite elements characterized by the duality in energy of tractions and displacement discontinuities. The enriched formulation introduces also a constitutive correlation between the in-plane deformation (elongation or confinement) of the interface and the membrane state of stress, as proposed even in [9]. This assumption permits to easily translate at the interface level the constitutive laws of the continuum. An interface damage model which accounts for the mode I and mode II and the axial deformation of the interface is proposed starting by the use of Drucker-Prager failure criterion. Simple numerical simulations are presented in order to illustrate the capabilities of the model. Later on, some numerical applications are carried out in order to assess the performances of the proposed model in reproducing the mechanical behaviour of masonry elements strengthened with external FRP reinforcements. In particular, the effects of mortars joints in masonry substrate reinforced with FRP is investigated.

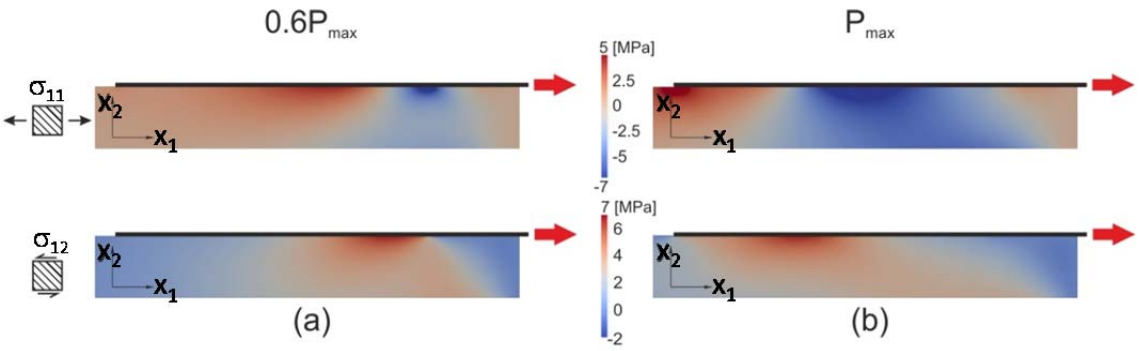

Figure 1: Finite Element simulation of the debonding tests in [8] ; (a) stresses in the substrate at 60% of the maximum force ; (b) stresses in the substrate at the maximum force.

2 ENRICHED INTERFACE MODEL

In this section, the kinematically enriched interface model is presented in the framework of the small displacement and strain regime [10]. In the following the Voigt notation is adopted, so that strain and stress are represented in vectors. The analysis is developed in 2D case.

A thin layer Ω with cross-section S and constant small thickness t is considered. A local cartesian reference system (x_1, x_2) is introduced, with x_2 orthogonal to S, as illustrated in Figure 2.

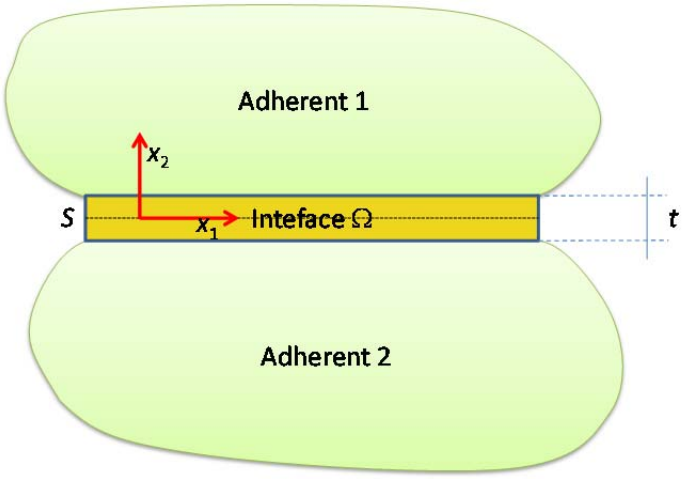

Figure 2: Geometrical scheme of the interface and coordinate system.

The displacement vector is denoted as $\mathbf{u} = \{u_1 \quad u_2\}^T$, so that the displacement vectors evaluated at the top and bottom of the interface, i.e. at $x_2 = t/2$ and $x_2 = -t/2$, are indicated by $\mathbf{u}^+$ and $\mathbf{u}^-$, respectively.

Adopting the Voigt notation, the strain is organized in the vector:

$$\boldsymbol{\varepsilon} = \{\varepsilon_{11} \quad \varepsilon_{22} \quad \gamma_{12}\}^T \tag{1}$$

with

$$\varepsilon_{11} = u_{1,1} \quad \varepsilon_{22} = u_{2,2} \quad \gamma_{12} = u_{1,2} + u_{2,1} \tag{2}$$

where the comma indicates the partial derivative.

Due to the smallness of the interface thickness, the derivatives along the x_2 direction can be evaluated as the difference between the values at the top and bottom of the interface, i.e. it is set $u_{2,2} = s_2 / t$ and $u_{1,2} = s_1 / t$, with s_1 and s_2 the components of the relative displacement defined as $\mathbf{s} = \mathbf{u}^+ - \mathbf{u}^-$. On the basis of the above assumption, and neglecting the derivative $u_{2,1}$ which represents a micro-rotation of the interface cross-section S, the strain components multiplied by the thickness t can be represented in the form:

$$\boldsymbol{\varepsilon} t = \mathbf{c} = \begin{Bmatrix} \overline{u}_{1,1} t \\ s_2 \\ s_1 \end{Bmatrix} \tag{3}$$

Concerning the constitutive response of the interface, it is subjected to damage effect; thus, according to Continuum Damage Mechanics the stress-displacement vector relationship reads:

$$\boldsymbol{\sigma} = (1 - D)\mathbf{K}\mathbf{c} \tag{4}$$

where D is the damage variable and $\mathbf{K}$ is a diagonal matrix containing the elastic stiffness parameters of the interface. For the considered case, the terms of $\mathbf{K}$ are the classical interface stiffness coefficients for sliding and opening mechanisms and the parameter associated to the elongation which depends on the elastic modulus of the substrate. The kinematical assumption permits to easily translate at the interface level the constitutive laws of the continuum.

Concerning the damage evolution process, different criteria can be adopted for the proposed interface model. An interface damage model which accounts for the mode I and mode II and the axial deformation of the interface is proposed starting by the use of Drucker-Prager failure criterion in the form:

$$f = \overline{\sigma}_{eq} - k \le 0 \tag{5}$$

where $\overline{\sigma}_{eq}$ is the equivalent stress, defined as:

$$\overline{\sigma}_{eq} = s_d + \alpha s_m \tag{6}$$

with s_m and s_d the first invariant of $\overline{\boldsymbol{\sigma}}$ and the second invariant of the deviatoric part of $\overline{\boldsymbol{\sigma}}$ being $\overline{\boldsymbol{\sigma}} = \mathbf{K}\mathbf{c}$ the so-called effective stress.

The constants α and k depends on the mechanical properties of materials and can be determined from experimental tests. Since the Drucker-Prager yield surface can be interpreted as a smooth version of the Mohr-Coulomb yield surface, α and k can be expressed in terms of the cohesion and the angle of internal friction that are used to characterized the Mohr-Coulomb yield surface.

Eq. (2) ensures that the yield condition is reached when $f = \overline{\sigma}_{eq} - k = 0$. Then, the stress-

displacement relationship is linear elastic for $\bar{\sigma}_{eq} < k$; when $\bar{\sigma}_{eq} = k$ a damage evolution occurs with linear softening in the stress-strain relation.

Denoting as k_u the ultimate value of the equivalent effective stress, for which the stress vector is trivial, the following evolution law of the damage parameter is assumed:

$$D = \max\left(0, \min\left(1, \tilde{D}\right)\right), \quad \text{with } \dot{D} \geq 0 \text{ being} \quad \tilde{D} = \frac{k_u\left(k - \bar{\sigma}_{eq}\right)}{\bar{\sigma}_{eq}\left(k - k_u\right)} \tag{7}$$

In order to estimate the interface parameters the simple case of pure shear is considered. In fact, it results $\bar{\sigma}_{eq} = \sigma_{12}$ and the damage evolution law(7), under the hypothesis of monotonic loading, becomes:

$$D = \frac{k_u\left(k - \bar{\sigma}_{12}\right)}{\bar{\sigma}_{12}\left(k - k_u\right)} \tag{8}$$

In this case, the constitutive relationship (4) reduces to:

$$\sigma_{12} = \left(1 - D\right)\frac{G}{t}s_1 \tag{9}$$

being G the shear modulus of the adhesive. Simple manipulation of Eq. (8) reveals that the stress component σ_{12} is a decreasing linear function of the sliding displacement s_1 during the damage evolution.

In short, the parameters of the damaging interface law are three; k defines the elastic domain, k_u specifics the complete damage state while α quantifies the influence of the membrane stress on the failure criterion.

The damage interface model presented in this section has been implemented into a four-node interface element, as described in [10]. Different parameters have been adopted at the interface level for the brick and the mortar joints. For the bulk materials, linear elastic two-dimensional plane-strain model and bilinear quadrilateral elements were adopted. The problem has been solved using a quasi-static incremental/iterative solution procedure. In order to follow the softening and snap-back branches of the structural response, an arc-length method has been used.

3 NUMERICAL SIMULATIONS

In order to investigate the influence of mortar joints in the debonding process of masonry brick two numerical tests have been conducted. The first one replicates the single lap shear experimental test proposed in[11] on handmade 19th century bricks reinforced by single layer CFRP. Later on we studied the effect of mortar joints on the effective anchorage length[12] by simulating the debonding process on a hypothetic prism with an extremely long bonded area.

3.1 Test 1

In reference [11] the masonry prisms were realized with lime mortar and four units. Joints thickness was about 10 mm and the reinforcement has been glued on the head of the bricks. A

nominal length of the bonded zone l_b=150 mm was chosen. The specimen geometry is illustrated in Figure 3a, while the principal mechanical parameters of the glue declared by the producer are: Young's modulus E_a=3000 MPa and tensile strength f_{ta}= 70.0 MPa. The average Young's modulus of the reinforcement measured during the tests and referred to the effective mean thickness $t_{f,eff}$ = 1.4mm is $E_{f,eff}$=63500 MPa. The mechanical properties (Young modulus E_m, Poisson ratio ν, compressive and flexural tensile strengths f_{cm} and $f_{tm,fl}$) of materials and the adopted interface parameters are reported in Table 1. The elastic domain in the plane σ_{11}–σ_{12} for the brick interface is plotted in Figure 3c for different values of the normal stress σ_{22}.

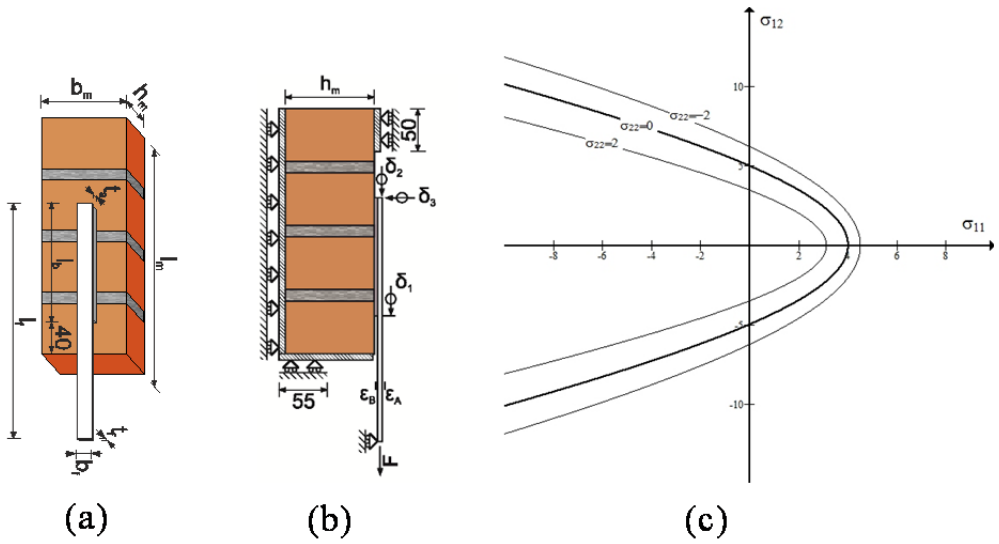

Figure 3: a) Geometry and b) structural scheme of the experimental test [11];
c) elastic domain adopted for the masonry substrate.

The problem was modeled in two dimensions. A scheme of the test, details and boundary conditions are showed in Figure 3b. Right side, top and bottom portions of the specimen are constrained in order to have no displacements in the direction normal to the surface and free displacements tangent to it.

Table 1: Mean values of the mechanical properties the material and adopted interface parameters for Test 1.

Material	E_m (MPa)	ν	f_{cm} (MPa)	$f_{tm,fl}$ (MPa)	k(MPa)	k_u (MPa)	α	t(mm)
Brick	8300	0.13	12.6	3.2	5	27.3	1.75	15
Mortar	7500	0.26	4.8	1.1	1.25	26.4	1.75	15

Numerical and experimental detachment curves are compared in Figure 3a. The simulation has been conducted also for a specimen made only of masonry. Numerical results are in good agreement with experimental data (considering the unavoidable scattering of the experimental results). The behavior for low load levels is well predicted, so assuring that initial (elastic) stiffness of the interface law is correctly estimated. The maximum value of the transmitted

force P_{max} is correctly predicted. The heterogeneities at the interface level causes drops in the reported equilibrium graph [13]. This phenomenon is correctly reproduced by the numerical simulation.

Stress profiles along the anchorage are reported in Figure 4b and Figure 5a-b. Curves refer to three different equilibrium points indicated by red dots in Figure 4a: load values $0.7P_{max}$, $P_{max,}$ and maximum displacement u_{max}.

The shear stress σ_{12} has discontinuous distribution at the joint level. The normal stress σ_{22} presents not negligible values near the joint position and at the end of the anchorage (i.e. x=0) once that the debonding has reached the back of the reinforcement.

The confinement stress σ_{11} is always in traction in Figure 4b while in the other two equilibrium points presents positive value before the peak of the shear stress and turns in compression in the damaged portion of the interface. From Figure 5a emerges how joint induces two local maximum points in the graph of the stress distribution in the bricks connected by the joints.

The local behavior at the interface level is investigated in Figure 6 and in Figure 7, where the stress components σ_{11}, σ_{12}, σ_{22} are plotted as a function of the slip s_1 in two different points of the bricks and in the joints. In both cases, it appears the influence of the confinement stress on the shear stress components. The influence is much higher at the joint level because the value of stress components σ_{11} and σ_{12} are similar.

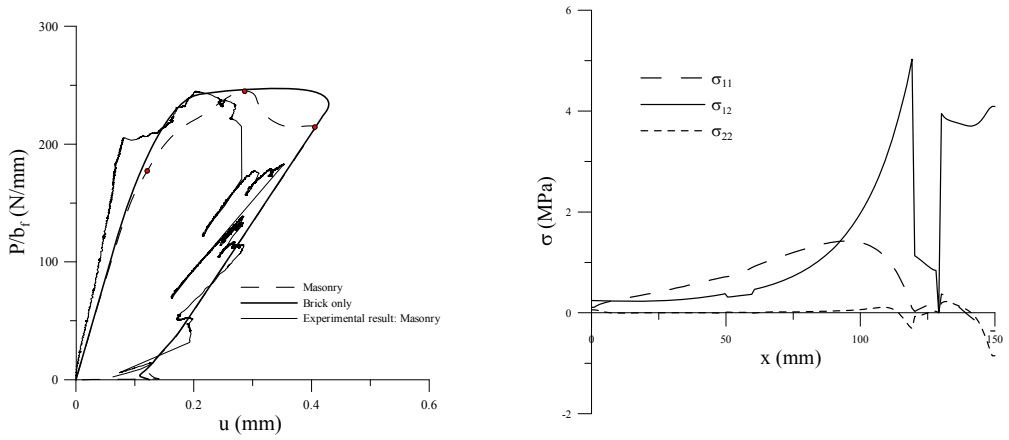

Figure 4: a) Detachment curves per unit width: experimental and numerical results, b) Stress distribution along the interface for $0.7P_{max}$.

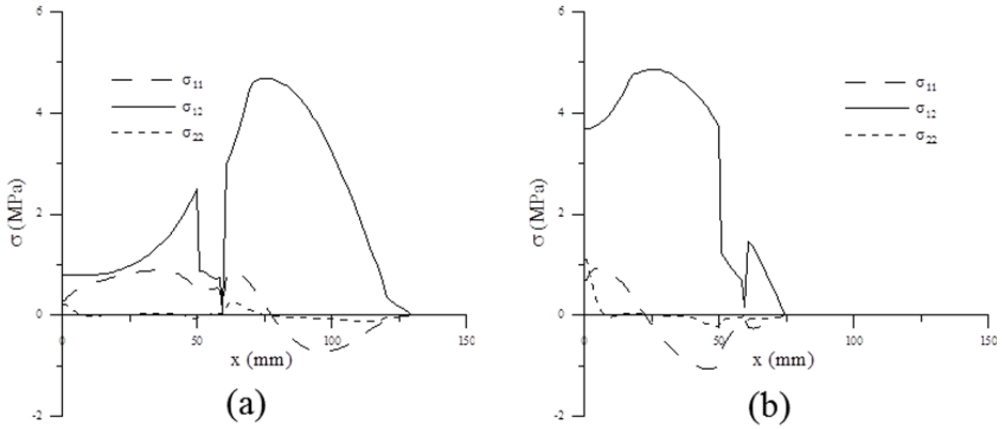

Figure 5: Stress distribution along the interface for a) P_{max}, b) u_{max}.

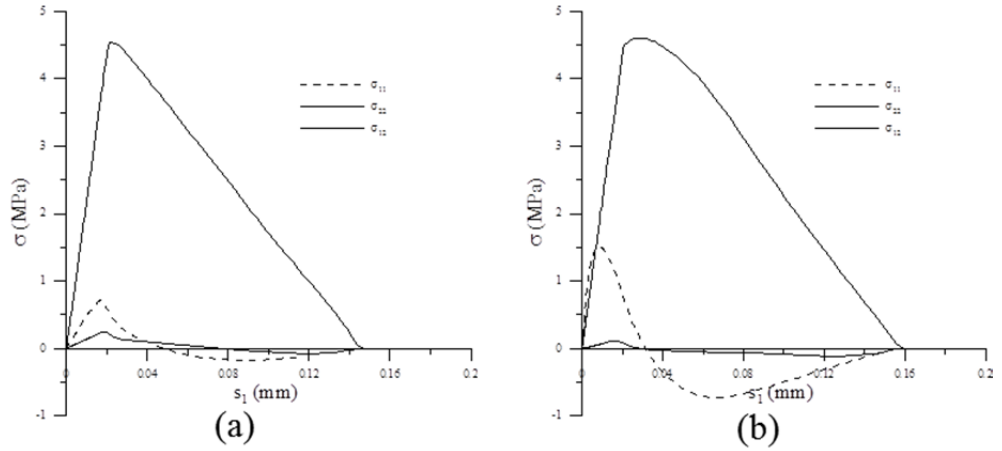

Figure 6: Local interface shear stresses vs slip $s_1$in bricks a) *x*=140mm, b) *x*=90mm.

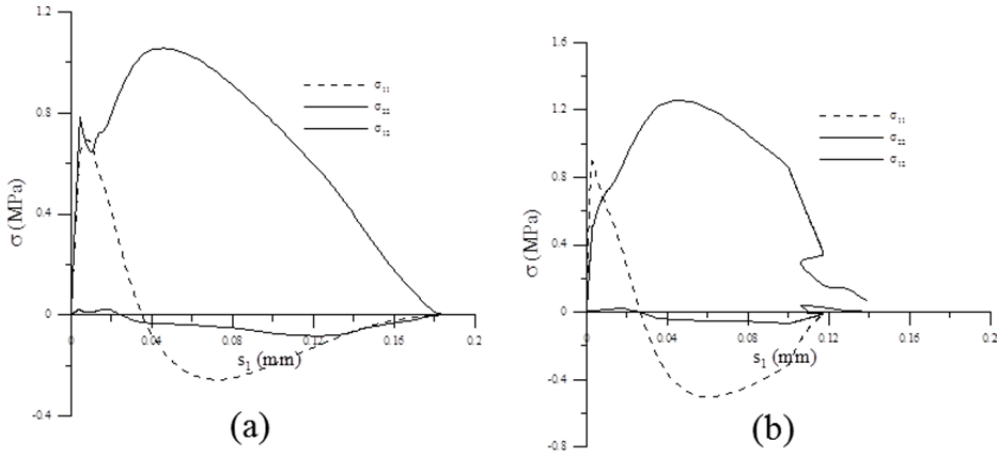

Figure 7: Local interface shear stresses vs slip s_1 located in joints: a) *x*=125mm, b) *x*=55mm.

3.2 Test 2

The second simulation replicates the setup of the previous example. In this case the specimen is much longer l_m=600 mm and length of the bonded zone l_b has been increased up to 500 mm. The substrate underneath the interface is now composed by 8 bricks and 7 joints. The material and interface properties have been left unchanged and are reported in Table 1 with the only exception of the Elastic modulus of the joint that now is E_m=3300MPa.

Figure 8a reports the detachment curves of the test together with the result in case brick only is considered. The global response evidences stable and unstable drops in the equilibrium path; one drop for each mortar joint. The maximum force value obtainable is higher than in the case of brick substrate but the drops are rather pronounced, thus leading to a medium value that is nearly 7% smaller than the transmitted force by brick. The stress distribution has been investigated at several critical equilibrium points that are indicated in Figure 8a. In the central drop three points have been considered: the two extremities (points D and F) and point E that is located at the middle of the snap-back branch. In Figure 8b -Figure 12 the stress components σ_{11}, σ_{12}, σ_{22} are plotted along the anchorage. The 10 mm thick mortar joints are located at positions x=10, 80, 150, 220, 290, 360 and 430 mm. In all cases the maximum points (A, C, D, G and I) are characterized by a peak of the shear stress component σ_{12} in the brick near the right side of the joint that is about to debond. Differently, the minimum points (B, F and H) present highest values of the shear stress in the brick just at the right side of the joint. The drop phase, as outlined by Figure 10b, presents a cut in the σ_{12} graph at the joint level. In all points the vertical stress $\sigma_{22}$is characterized by very limited value while the confinement stress play a non-negligible rule in the damaging process.

Moreover, from the diagrams it clearly appears that the joint contribution in the transferring process of shear stress is extremely limited. So, in the calculation of the effective anchorage length the joints should be not taken into account.

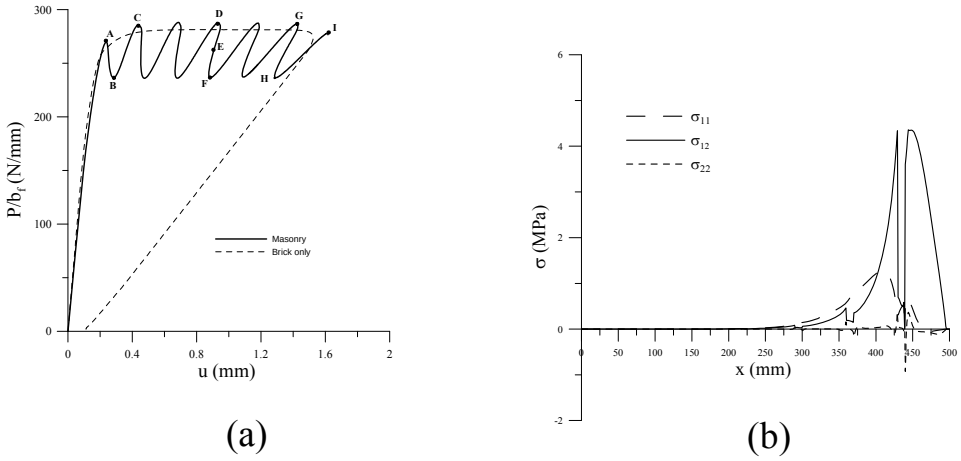

Figure 8: a) Detachment curves per unit width. b) Stress distributions along the interface at point A of Figure 8a).

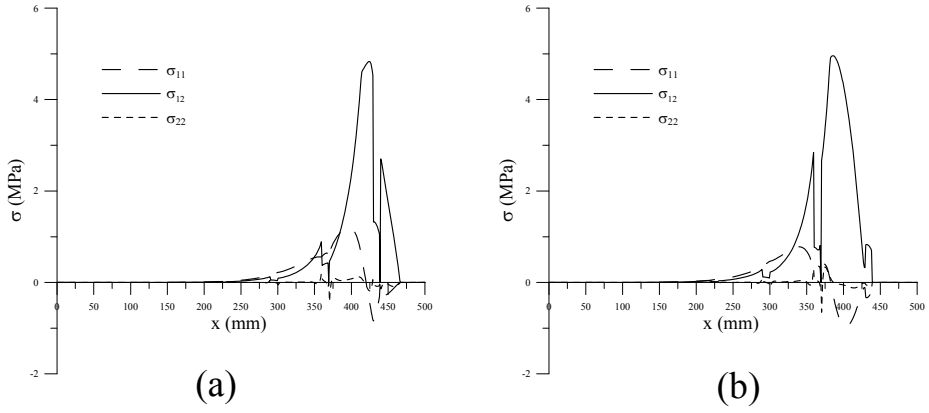

Figure 9: Stress distributions along the interface a) Point B, b) Point C of Figure 8a.

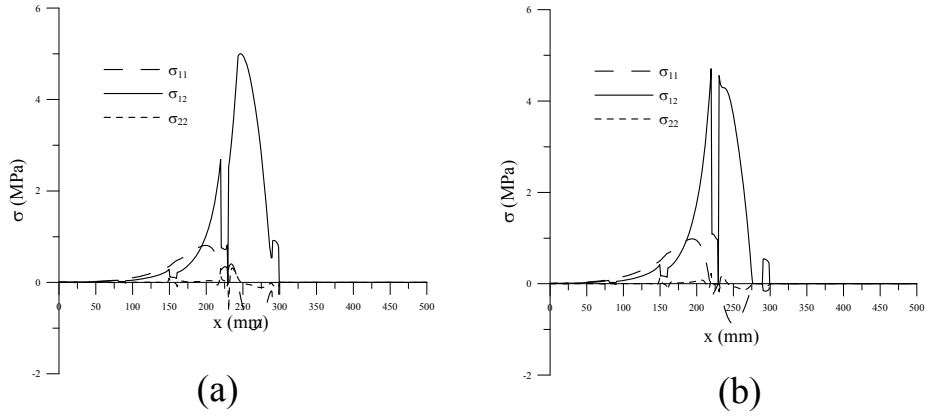

Figure 10: Stress distributions along the interface a) Point D, b) Point E of Figure8a.

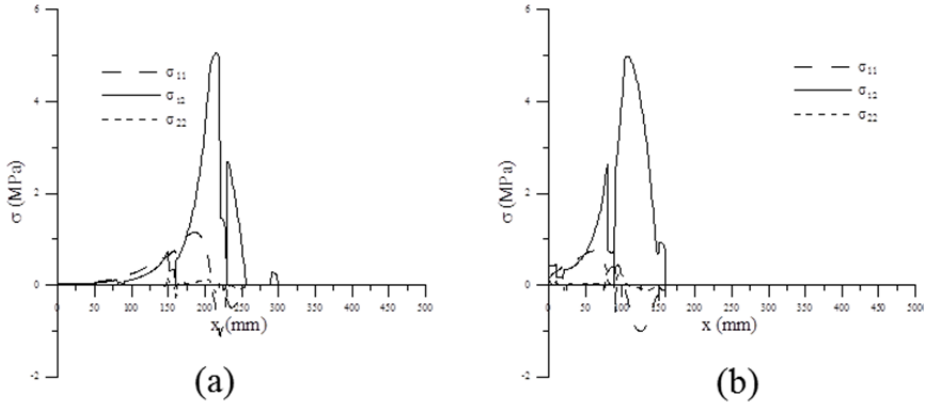

Figure 11: Stress distributions along the interface a) Point F, b) Point G of Figure8a.

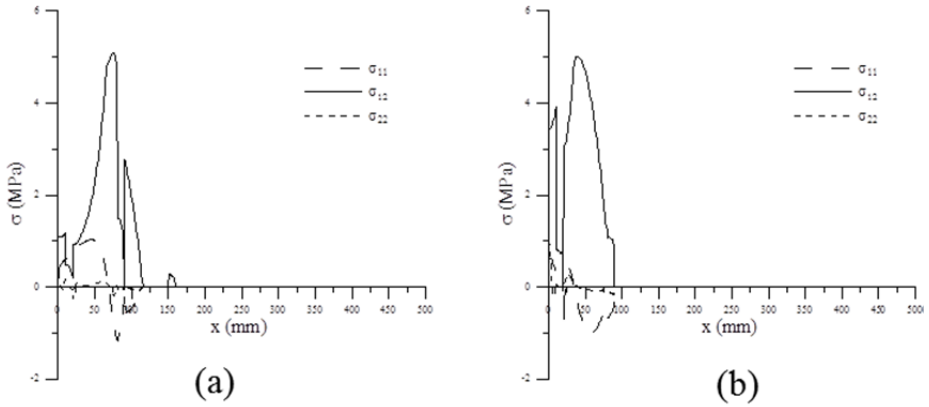

Figure 12: Stress distributions along the interface a) Point H, b) Point I of Figure8a.

4 CONCLUSIONS

An enhanced formulation for cohesive interface that keep into account the effect of in-plane deformations of the gluing surface has been developed.

The proposed model has been used to study the debonding mechanism of the FRP from a masonry support. In particular, the influence of the presence of mortar joints in the masonry texture is numerically investigated.

Load drops, commonly obtained in the experimental response and associated with the presence of mortar joints, are reproduced numerically. From the analysis, it can be noticed that the load drop is influenced by the mortar joint stiffness and strength. The load drop occurs when the mortar joint is involved in load transfer. As the load-carrying capacity of the mortar interface is lower than that of the brick a decrease in the overall load carrying capacity results from a longer portion of the transferring zone corresponding to the mortar joint.

Finally, it can be remarked that averaging the force-displacement curve (Figure 8a) during the decohesion phase, it can be remarked a reduction of the overall resistance of the masonry (with mortar joints) with respect to the behavior obtained considering the solely brick. The reduction of the carried load is accordance with the prescription of the document CNR DT200 [14], which suggest a reduction of 15% of the debonding load in presence of mortar joints.

ACKNOWLEDGMENTS

This research has been possible thanks to the financial supportof the project ReLUIS from the Italian Ministry of the CivilProtection.

REFERENCES

[1] M. R. Valluzzi, D. V. Oliveira, A. Caratelli, G. Castori, M. Corradi, G. de Felice, E. Garbin, D. Garcia, L. Garmendia, E. Grande, U. Ianniruberto, A. Kwiecień, M. Leone, G. P. Lignola, P. B. Lourenço, M. Malena, F. Micelli, M. Panizza, C. G. Papanicolaou, A. Prota, E. Sacco, T. C. Triantafillou, A. Viskovic, B. Zając, G. Zuccarino, Round Robin Test For Composite-To-BrickShear Bond Characterization. *Materials and Structures RILEM*, 45: 1761-1791, (2012).

[2] P. Carrara, F. Freddi., Statistical assessment of a design formula for the debonding resistance of

FRP reinforcements externally glued on masonry units, *submitted to Composites Part B: Engineering*, (2014).
[3] F. Freddi, M. Frémond, Damage in domains and interfaces: a coupled predictive theory. *Journal of Mechanics of Materials and Structures*, 1, 1205-1234, (2006).
[4] S. Marfia, E. Sacco, J. Toti, A coupled interface-body nonlocal damage model for FRP strengthening detachment.*Computational Mechanics*, 50, 335-351, (2012).
[5] J. Toti, S. Marfia, E. Sacco, Coupled body-interface nonlocal damage model for FRP detachment. *Comput. Methods Appl. Mech. Engrg.* 260, 1–23, (2013).
[6] B. Ferracuti, M. Savoia, and C. Mazzotti, A numerical model for FRP–concrete delamination. *Composites Part B: Engineering*, 37, 356–364, (2006).
[7] K. Benzarti, F. Freddi, M. Frémond, A damage model to predict the durability of bonded assemblies. Part I: Debonding behavior of FRP strengthened concrete structures. *Construction and Building Materials*, 25, 547-555, (2011).
[8] P. Carrara, D. Ferretti, F. Freddi, and G. Rosati, Shear tests of carbon fiber plates bonded to concrete with control of snap-back, *Engineering Fracture Mechanics*, 78, 2663–2678, (2011).
[9] G. Giambanco, G. Fileccia Scimeni, and A. Spada, The interphase finite element *Computational Mechanics*, 50, 353–366, (2012).
[10] F. Freddi, E. Sacco, An interface damage model depending on the deformation of the adherent.*In preparation* (2014).
[11] P. Carrara, D. Ferretti, F. Freddi, Debonding behavior of ancient masonry elements strengthened with CFRP sheets, *Composites Part B: Engineering*, 45(1): 800-810, (2013)
[12] B. Ghiassi, D. V. Oliveira, P.B. Lourenço, G. Marcari, Numerical study of the role of mortar joints in the bond behavior of FRP-strengthened masonry, *Composites Part B: Engineering*, 46 (2013) 21-30.
[13] C. Carloni,K. Subramaniam, FRP-Masonry Debonding: Numerical and Experimental Study of the Role of Mortar Joints, *J. Compos. Constr*., 16(5), 581–589. (2012)
[14] CNR DT200 *Guide for the design and construction of an externally bonded FRP system for strengthening existing structures*. Italian National Research Council, Rome (2004/2013)